Quaternary Science Reviews 197 (2018) 246–256

Contents lists available at ScienceDirect

Quaternary Science Reviews

journal homepage: www.elsevier.com/locate/quascirev

An Icelandic terrestrial record of North Atlantic cooling c. 8800–8100 cal. yr BP

Sigrún Dögg Eddudóttir [a, *], Egill Erlendsson [a], Guðrún Gísladóttir [a, b]

[a] Institute of Life and Environmental Sciences, University of Iceland, Sturlugata 7, 101 Reykjavík, Iceland
[b] Institute of Earth Sciences, University of Iceland, Sturlugata 7, 101 Reykjavík, Iceland

ARTICLE INFO

Article history:
Received 4 May 2018
Received in revised form
6 July 2018
Accepted 9 July 2018
Available online 25 August 2018

Keywords:
Climate change
Vegetation dynamics
Pollen
8.2 ka event
Palaeoclimate
North Atlantic
Iceland
Holocene
Lake sediment

1. Introduction

Iceland's location in the North Atlantic makes the terrestrial environment of the island sensitive to changes in atmospheric and oceanic systems in the region. The terrestrial ecosystem is particularly responsive to changes in ocean currents since the island is located at the junction of the relatively warm Irminger Current and the colder East Greenland Current (e.g. Stefánsson, 1962; Hansen and Østerhus, 2000). Palaeoenvironmental reconstructions from Icelandic lake sediments have revealed centennial and millennial scale environmental responses to climate change during the Holocene (Hallsdóttir, 1995; Rundgren, 1998; Hallsdóttir and Caseldine, 2005; Geirsdóttir et al., 2009, 2013; Larsen et al., 2011, 2012; Striberger et al., 2012; Blair et al., 2015; Eddudóttir et al., 2015, 2016; Schomacker et al., 2016). A prominent anomaly in some Icelandic palaeoenvironmental reconstructions is a cold period between c. 8700–7900 cal. yr BP, interrupting a trend of warming climate during the early Holocene (Geirsdóttir et al., 2009, 2013; Larsen et al., 2012; Eddudóttir et al., 2015). The cooling during this period is evident from proxies sensitive to changes in spring and summer temperatures and is reflected in changes in both terrestrial vegetation (Eddudóttir et al., 2015) and lake productivity (Larsen et al., 2012). The cooling observed in Iceland falls within the period c. 9000–8000 cal. yr BP, which is characterised by cold conditions in the Northern Hemisphere (Mayewski et al., 2004), and coincides with a cold anomaly beginning c. 8600 cal. yr BP recorded around the North Atlantic (cf. Rohling and Pälike, 2005). This longer cold period is distinct from the cold anomalies related to the 8.2 ka cold event (e.g. Alley et al., 1997; Baldini et al., 2002; Alley and Ágústsdóttir, 2005; Rohling and Pälike, 2005; Bamberg et al., 2010), which has been linked to the flux of meltwater at the final drainage of the glacial lakes Agassiz and Ojibway into the North Atlantic c. 8430 ± 300 cal. yr BP (Barber et al., 1999).

The timing and nature of terrestrial ecosystem changes in Iceland can highlight the nature of centennial scale climate fluctuations in the North Atlantic and provide information to complement marine records. The aim of this study was to create a detailed record of environmental changes in northwestern Iceland in response to early Holocene climate change. Here we present a palynological reconstruction of the period c. 10,100–7000 cal. yr BP. To establish whether changes in environmental stability occurred during this period the multi-decadal resolution palynological dataset is supplemented by plant macrofossils and measurements of organic and physical properties of the sediment, including organic matter (OM), total carbon (TC), total nitrogen (TN), carbon-to-nitrogen ratio (C/N), stable isotope ratios of carbon ($\delta^{13}C$) and nitrogen ($\delta^{15}N$), magnetic susceptibility (MS) and dry bulk density (DBD).

2. Regional setting

The site chosen for this study is Kagaðarhóll palaeolake (KAGA; 65°35′ 16″ N, 20°07′ 58″ W, 114 m a.s.l.) located in northwest Iceland, about 10 km south of the town of Blönduós (Fig. 1). The palaeolake is today a fen and is about 0.45 km^2 in area, with a drainage basin of about 0.6 km^2. The vegetation is dominated by sedges (Cyperaceae spp.), especially *Eriophorum angustifolium* (common cotton grass), the dwarf shrubs *Betula nana* (dwarf birch), *Salix phylicifolia* (tea-leaved willow) and *Salix lanata* (woolly

* Corresponding author.
E-mail address: sde6@hi.is (S.D. Eddudóttir).

https://doi.org/10.1016/j.quascirev.2018.07.017
0277-3791/© 2018 Elsevier Ltd. All rights reserved.

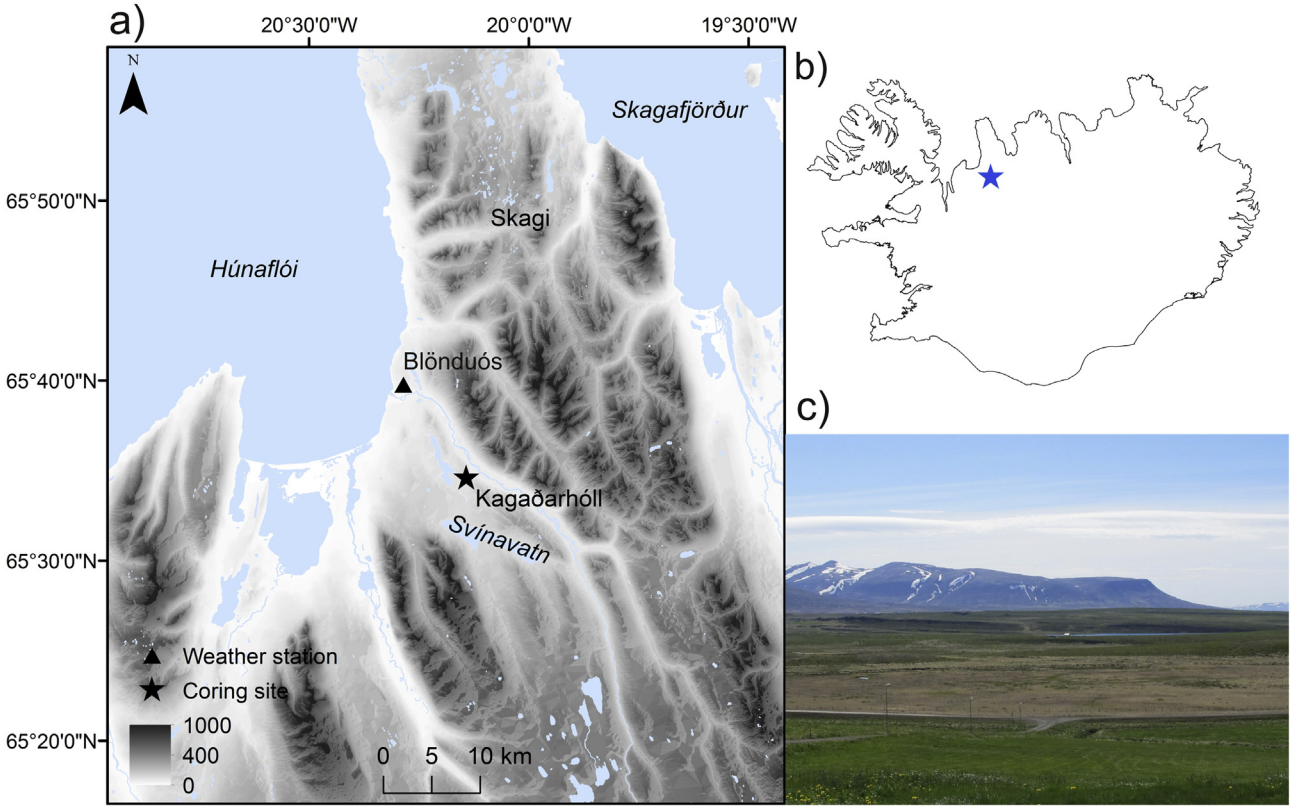

Fig. 1. The Kagaðarhóll study site. a) Map showing the location of the coring site in northwest Iceland, b) map of Iceland showing the location of Kagaðarhóll and, c) overview of the palaeolake.

willow), and the herb *Cardamine nymanii* (lady's smock). The overgrown lake is surrounded by *Betula nana*-dominated dwarf-shrub heath, hayfields and eroded, gravelly hills. The closest weather station is Blönduós (Table 1), which is located by the coast and may therefore represent a more maritime climate than Kagaðarhóll. For more detailed site information see (Eddudóttir et al., 2015, 2017).

3. Material and methods

Sediment cores were retrieved from the centre of the palaeolake using a Livingstone piston corer and a Bolivia adaptor fitted with 75 mm diameter polycarbonate tubes. A series of overlapping cores was used to construct a continuous Holocene sequence with 0 cm at the top of the core (see Eddudóttir et al., 2015). The period c. 10,100–7000 cal. yr BP is covered by three overlapping core segments connected by changes in magnetic susceptibility (MS) and tephra geochemistry (Fig. S1). A description of sediment characteristics according to the Troels-Smith system (Aaby and Berglund, 1986) is presented in Table S1.

The pollen dataset consists of 46 samples, covering the period c. 10,100–7000 cal. yr BP, comprising 31 samples previously analysed as part of a dataset published in Eddudóttir et al. (2015) and 15 new samples. Subsamples for pollen analysis (2 cm^3) were collected at 2–8 cm intervals. Pollen samples were prepared using 10% HCl, 10% NaOH, acetolysis (Faegri et al., 1989; Moore et al., 1991) and dense-media separation (Björck et al., 1978; Nakagawa et al., 1998) using LST Fastfloat (a sodium heteropolytungstate solution, density 1.9 g cm^{-3}). A tablet containing spores of *Lycopodium clavatum* (Stockmarr, 1971; batch no. 177745) was added to each sample to calculate pollen accumulation rates (PARs; grains cm^{-2} $year^{-1}$). Samples were mounted on glass microscope slides in silicone oil of 12,500 cSt viscosity. A minimum of 300 indigenous terrestrial pollen grains were counted for each sample. Identification of pollen grains and spores was based on Moore et al. (1991) and a pollen type slide collection at the University of Iceland. Pollen sums and categories followed Hallsdóttir (1987) and Caseldine et al. (2006). Pollen and spore taxonomy followed Bennett (2016) and amendments specific to the Icelandic flora by Erlendsson (2007). The sediments were analysed for plant macrofossils at contiguous 5 cm intervals and sample volume varied between 35 and 50 mL (for further detail see Eddudóttir et al. (2015)). Pollen and macrofossil diagrams were constructed using TILIA version 1.7.16 (Grimm, 2011).

Table 1
Observations from the weather station Blönduós. Unpublished data from the Icelandic Met Office.

Elevation	8 m a.s.l.
Period	1961–1990
Mean July temperature	9.4 °C
Mean January temperature	−2.5 °C
Mean tritherm temperature (mean June, July, August temperature)	8.7 °C
Mean annual precipitation	458 mm

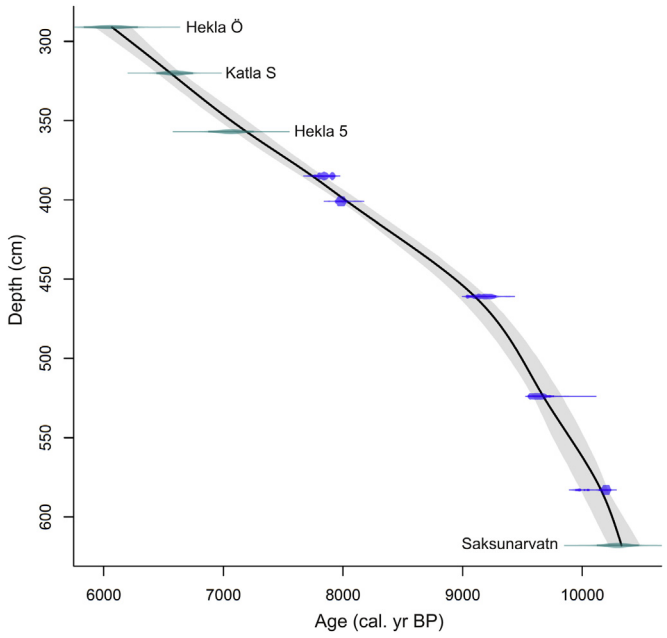

Fig. 2. Age-depth model for the Kagaðarhóll core.

DBD and OM were measured at 1 cm contiguous intervals. OM was measured by loss on ignition (LOI) by combustion for 5 h at 550 °C in a muffle furnace (Bengtsson and Enell, 1986) and DBD was calculated by dividing the dry weight of a sample with the volume of the wet sample (Brady and Weil, 1996). Magnetic susceptibility (MS) measurements were performed using a Bartington MS2 meter and Bartington MS2F probe (Dearing, 1994) at 1 cm intervals on split core segments.

The core was subsampled for measurements of total carbon (TC), total nitrogen (TN) and $\delta^{13}C$ and $\delta^{15}N$ stable isotope ratios of bulk sediments at the same depths as the pollen samples, where possible. The samples were dried at 50 °C, homogenized using a ball mill and sieved through a 150 μm mesh. A total of 46 samples were analysed. The carbon, nitrogen and isotope measurements were performed on a Thermo Delta V isotope ratio mass spectrometer (IRMS) interfaced to a NC2500 elemental analyser at the Cornell University Isotope Laboratory (COIL).

The chronology for the Kagaðarhóll core (Fig. 2) was constructed using a combination of tephrochronology and radiocarbon dates (Eddudóttir et al., 2015). The age-depth model for the core (Fig. 2) is based on the previously dated tephra layers Hekla Ö (6060 cal. yr BP; Gudmundsdóttir et al., 2011), Katla S (6600 cal. yr BP; Eddudóttir et al., 2015), Hekla 5 (7050 cal. yr BP; Thorarinsson, 1971) and Saksunarvatn (10,300 cal. yr BP; Rasmussen et al., 2006) and radiocarbon dated macrofossils (Table 2). A smooth spline age-depth model (Fig. 2) was constructed in R using the package Clam (Blaauw, 2010). Ages are given in calibrated years before present (cal. yr BP). According to the 95% confidence of the age model the age uncertainty is ±100–120 yrs for most of the record; lowest c. 8600–7400 cal. yr BP (≤± 100 yr) and highest (±120–130 yrs) c. 10,100–9700 cal. yr BP.

Ordination analyses were performed on the pollen dataset to detect patterns in terrestrial vegetation development in the vicinity of the lake. Detrended correspondence analysis (DCA) was initially used. As the first axis length of 1.3527 suggests a linear response in the dataset, a principal component analysis (PCA) was preferred. The PCA was performed on a Hellinger transformed dataset that included terrestrial pollen taxa with abundances >1%. PCA analysis was also performed on a standardised dataset of %TC, %TN, %OM, C/N, MS, DBD, $\delta^{13}C$ and $\delta^{15}N$ along with the most important pollen groups and taxa (*Betula*, *Juniperus communis*, shrubs, herbs and aquatics) to determine the relationships between vegetation and sediment properties. This analysis includes 42 samples analysed for both pollen and organic and physical properties. All ordination analyses were made in R using the package vegan (Oksanen et al., 2016).

4. Results

4.1. Pollen assemblage zones (PAZs)

The pollen record covers the period c. 10,100–7000 cal. yr BP and is divided into five pollen assemblage zones (PAZs) based on CONISS performed in TILIA (Fig. 3).

PAZ 1 (10,100–9600 cal. yr BP)

Juniperus communis pollen is ~15–32% of total land pollen (TLP), *Betula* is ~14–32% of TLP and Cyperaceae is ~16–24% of TLP. Other important pollen types are *Empetrum nigrum* (~1–10% of TLP), *Salix* (~3–11% of TLP), *Galium* (~0.3–6% of TLP) and *Thalictrum alpinum* (~3–9% of TLP) (Fig. 3). The *Juniperus communis* PAR increases to >600 grains cm^{-2} yr^{-1} c. 9800 cal. yr BP (Fig. 4). Mean *Betula* pollen diameters are ~17 ± 1 μm within this PAZ (Fig. 5). *Potamogeton natans*-type pollen (~18–82% of total pollen and spores) is the most important aquatic pollen taxon (Fig. 3). *Selaginella selaginoides* megaspores and *Potamogeton natans* seeds along with *Luzula* and *Carex nigra* seeds are the most common plant macrofossils recorded within this PAZ (Fig. 6). Non-triporate *Betula* pollen range between 2 and 9% (Fig. 4).

PAZ 2 (9600–9200 cal. yr BP)

Juniperus communis pollen increases to ~38–58% of TLP and Cyperaceae decreases to ~4–13% of TLP. *Betula* ranges between 14 and 30% of TLP. *Galium* and *Thalictrum alpinum* pollen decrease within this PAZ, along with *Empetrum nigrum* and *Potamogeton natans*-type pollen. *Isoëtes echinospora* spores appear c. 9500 cal. yr BP (Fig. 3). The relative abundance of *Juniperus communis* pollen increases after c. 9600 cal. yr BP and the PAR is ~1300–3200 grains cm^{-2} yr^{-1} between c. 9600 and 9200 cal. yr BP. This period delivers the highest TLP PAR in the record (~3200–6400 grains cm^{-2} yr^{-1}), as well as high TLP concentration (~26,000–50,000 grains cm^{-3}; Fig. 4). Mean *Betula* pollen diameters are ~18 ± 1 μm within this PAZ (Fig. 5). *Betula nana* seeds and leaves and *Selaginella selaginoides* megaspores are the most common plant macrofossils recorded.

Table 2
Radiocarbon dates from the Lake Kagaðarhóll sediment.

Lab code	Depth (cm)	^{14}C date ± 1σ	$\delta^{13}C$	Calibrated age range	Material
ETH-56125	385	7003 ± 36	−20.6	7934–7751	*Potamogeton* leaf fragments
ETH-56126	401	7170 ± 35	−35.0	8033–7937	*Empetrum nigrum* and *Betula pubescens* various items
ETH-56135	461	8209 ± 38	−19.1	9280–9031	*Potamogeton* leaf fragments
ETH-56129	524	8695 ± 38	−11.7	9761–9546	*Potamogeton* fruits and leaf fragments
ETH-56130	583	8997 ± 39	−11	10,240–9942	*Potamogeton* fruits and leaf fragments

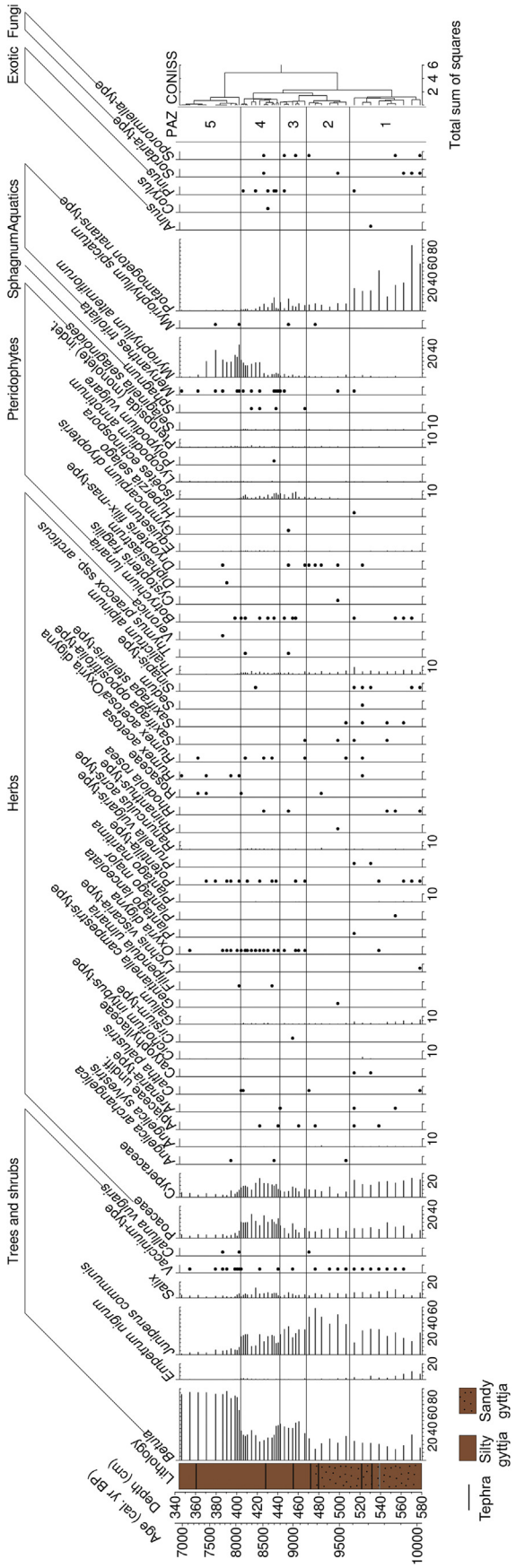

Fig. 3. Pollen percentage diagram for the Kagaðarhóll core.

Betula pubescens macrofossils appear at the top of this PAZ (Fig. 6). Non-triporate *Betula* pollen range between 2 and 5% (Fig. 4).

PAZ 3 (9200–8800 cal. yr BP)

Juniperus communis pollen decreases within this PAZ to ~22–35% of TLP and *Betula* pollen increases to ~34–49% of TLP. Pollen of *Oxyria digyna* and *Potentilla*-type appear within this PAZ but remain <1% (Fig. 3). The *Juniperus communis* PAR decreases to <900 grains cm^{-2} yr^{-1} c. 9100 cal. yr BP, and the *Betula* PAR increases to >1000 grains cm^{-2} yr^{-1} after c. 9200 cal. yr BP (Fig. 4). Mean *Betula* pollen diameters increase to ~20 ± 1 μm (Fig. 5). *Betula pubescens* macrofossils are abundant within this PAZ (Fig. 6). Non-triporate *Betula* pollen range between 2 and 7% (Fig. 4).

PAZ 4 (8800–8100 cal. yr BP)

Betula pollen decreases after c. 8700 cal. yr BP to <32% of TLP and *Juniperus communis* pollen continues to decrease to ~11–26% of TLP. Poaceae pollen increases to >20% of TLP c. 8800 cal. yr BP and Cyperaceae to >16% of TLP c. 8700 cal. yr BP (Fig. 3). The *Betula* PAR decreases to <600 grains cm^{-2} yr^{-1} after c. 8800 cal. yr BP and <200 grains cm^{-2} yr^{-1} after c. 8500 cal. yr BP. The TLP PAR decreases to <1400 grains cm^{-2} yr^{-1} c. 8800 cal. yr BP and <900 grains cm^{-2} yr^{-1} c. 8500 cal. yr BP (Fig. 4). Mean *Betula* pollen diameters are ~20 ± 1 μm within this PAZ (Fig. 5). *Myriophyllum alterniflorum* pollen increases while *Potamogeton natans*-type pollen decreases (Fig. 3). *Myriophyllum alterniflorum* seeds are the most common plant macrofossils within this PAZ (Fig. 6). Non-triporate *Betula* pollen range between 1 and 10% (Fig. 4).

PAZ 5 (8100–7000 cal. yr BP)

Betula pollen increases rapidly between c. 8100 and 8000 cal. yr BP from ~37% TLP c. 8100 cal. yr BP to ~79% TLP c. 8000 cal. yr BP. *Juniperus communis* pollen decreases dramatically within this PAZ to ~1–9% of TLP. Other pollen taxa such as Poaceae, Cyperaceae, *Salix*, *Thalictrum alpinum* and *Empetrum nigrum* decrease. *Galium* pollen disappears along with *Selaginella selaginoides* spores (Fig. 3). The *Betula* PAR is high from c. 8000 cal. yr BP (~1500–2500 grains cm^{-2} yr^{-1}) and the TLP PAR is ~1800–3200 grains cm^{-2} yr^{-1} (Fig. 4). Mean *Betula* pollen diameters are ~21 ± 1 μm (Fig. 5). *Betula pubescens* catkin scales and fruits and *Myriophyllum alterniflorum* seeds are the most abundant plant macrofossils in this PAZ (Fig. 6). Non-triporate *Betula* pollen range between 2 and 5% (Fig. 4).

4.2. Principal component analysis of pollen data

The first PCA axis accounts for 66.5% of the variance in the dataset and the second axis for 12.6%. The terrestrial pollen assemblage in PAZ 1 (c. 10,100–9600 cal. yr BP) is influenced by *Empetrum nigrum,* Poaceae, Cyperaceae, *Thalictrum alpinum* and *Galium*. *Juniperus communis* is the dominant pollen type in PAZ 2 (c. 9600–9200 cal. yr BP), however the influence of *Betula* pollen increases in PAZ 3 (c. 9200–8800 cal. yr BP). *Empetrum nigrum,* Poaceae, Cyperaceae, *Thalictrum alpinum* and *Galium*, as well as *Oxyria digyna* show a strong influence on the pollen assemblages within PAZ 4 (c. 8800–8100 cal. yr BP). *Betula* becomes the dominant pollen taxon within PAZ 5 (c. 8100–7000 cal. yr BP) (Fig. 7).

4.3. Organic matter and physical properties

MS and DBD values are high (DBD 0.16–0.34 g cm^{-3}, excluding tephra layers) between c. 10,100 and 9300 cal. yr BP (PAZ 1 and 2). Values decrease after c. 9300 cal. yr BP and the lowest values for the

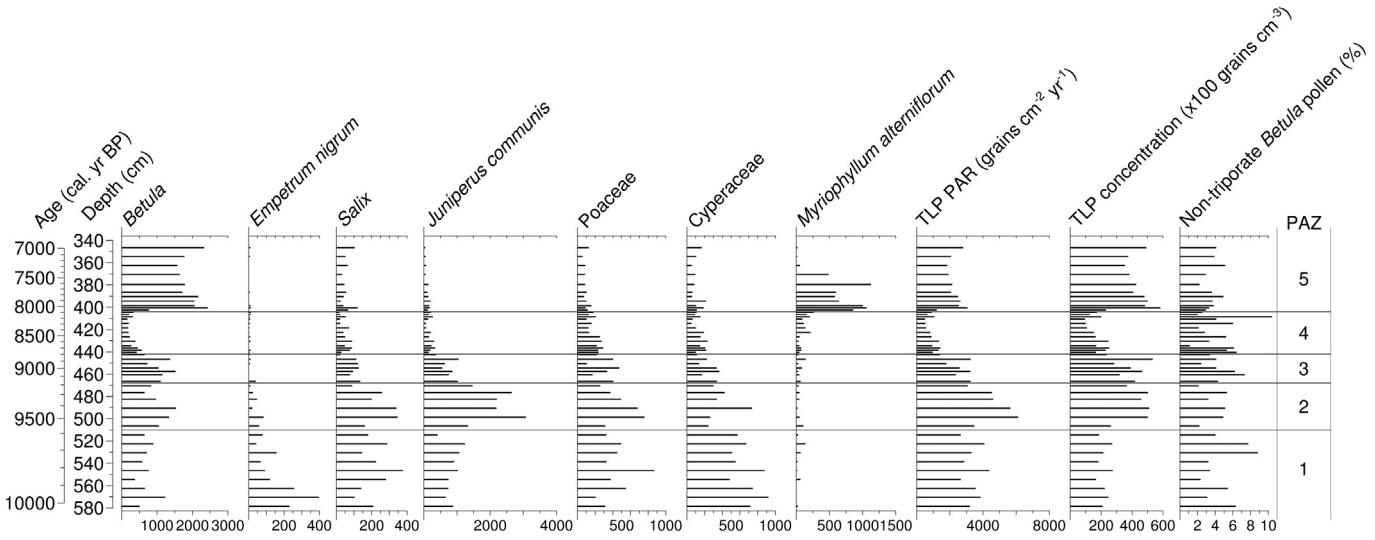

Fig. 4. Pollen accumulation rates of selected pollen taxa and TLP, concentration of TLP and percentage non-triporate *Betula* pollen.

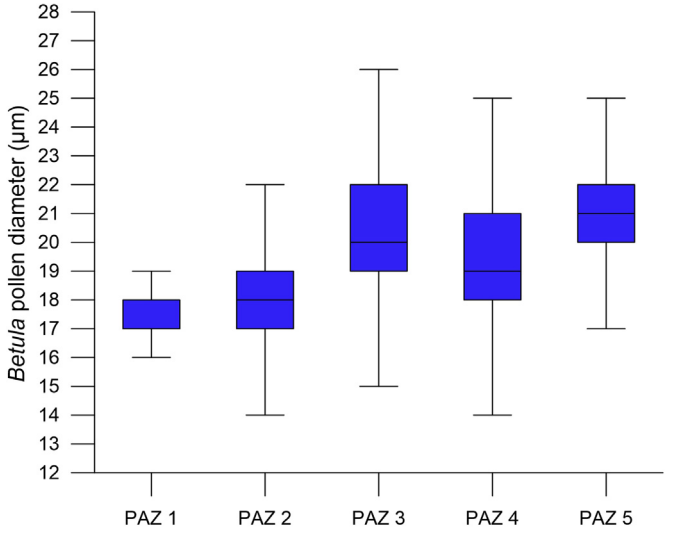

Fig. 5. Boxplot of *Betula* pollen grain diameters for each PAZ in the Kagaðarhóll record.

two proxies are recorded after c. 8500 cal. yr BP (DBD 0.09–0.19 g cm^{-3}). Organic matter proxies (%TC, %TN, C/N and %OM) increase with time. %TC increases from ~10–13% in PAZ 1 to >20% in PAZ 5. The C/N ratio increases from ~13% in PAZ 1 to ~15% in PAZ 5. The δ^{13}C isotope record shows decreased values with time, from ~−18‰ at c. 10,100 cal. yr BP to < −21‰ c. 9100 cal. yr BP. This trend is reversed after c. 8700 cal. yr BP and higher values (>−20‰) are recorded between c. 8400 and 8100 cal. yr BP. Values decrease to ~−21 and −23‰ after c. 8100 cal. yr BP (Fig. 8).

Although dissolved inorganic carbon (DIC) is found in rivers in Iceland (Kardjilov et al., 2006), the contribution of inorganic carbon to TC in Icelandic lake sediments is considered small due to the lack of carbonate bedrock (e.g. Langdon et al., 2010; Larsen et al., 2012; Jóhannesson, 2014; Harning et al., 2018) and changes in TC are considered to reflect changes in total organic carbon (TOC).

4.4. Principal Component Analysis of physical and organic matter properties and pollen

The first PCA axis accounts for 61.8% of the variance in the dataset and the second axis for 14.5%. High MS and DBD influence the samples in PAZs 1 and 2. Herb and shrub pollen, δ^{13}C, as well as aquatics are the dominant features in the samples in PAZ 1. In PAZ 2, *Juniperus communis* pollen and δ^{15}N are the most important factors influencing the samples. PAZ 3 is characterised by increased influence of *Betula* pollen and organic proxies (%OM, %TC and %TN), while the importance of the C/N ratio increases in PAZ 4. The dominant factors influencing the samples in PAZ 5 are *Betula* pollen and organic proxies (%OM, %TC, %TN and C/N) (Fig. 9).

5. Discussion

5.1. Early Holocene (c. 10,100–9200 cal. yr BP)

The pollen assemblage from Kagaðarhóll suggests the presence of *Juniperus communis-Betula nana-Salix* shrub heath for the first four centuries of the record (Fig. 3). This is supported by the dominance of pollen of *Juniperus communis* and *Betula* within PAZ 1. Other important pollen taxa are *Empetrum nigrum* and *Salix*, grasses (Poaceae), sedges (Cyperaceae), *Thalictrum alpinum* and *Galium* (Figs. 3 and 7). The presence of *Betula nana* is evidenced by small *Betula* pollen diameters ~17 ± 1 µm (Fig. 5) concurrent with modern *Betula nana* pollen (Mäkelä, 1996), as well as the presence of *Betula nana* macrofossils (Fig. 6). Macrofossils of heath taxa such as *Empetrum nigrum*, *Salix* spp., *Selaginella selaginoides* and graminoids (e.g. *Carex nigra* and *Luzula* spp.) support the presence of heath around the lake (Fig. 6).

The shrub heath was replaced by *Juniperus communis* scrub c. 9600 cal. yr BP, evidenced by a relative increase in *Juniperus communis* pollen to >38% of TLP (Fig. 3) and PARs of >1300 grains cm^{-2} yr^{-1} (Fig. 4). *Juniperus communis* is dominant in the TLP assemblage in PAZ 2. The high PAR of *Juniperus communis* pollen in the lake during this period indicates the presence of the upright growth form of the species around the lake (Eddudóttir et al., 2015). *Juniperus communis* produces large quantities of pollen (Huntley and Birks, 1983), but low amounts of pollen are found in lakes despite strong local presence (Birks and Bjune, 2010). However, high percentages and PARs of *Juniperus communis* can be produced by an upright growth form of dense scrub (Birks, 1973). Similar peaks in *Juniperus communis* pollen are also seen in other records from northern Iceland during this period (Hallsdóttir, 1995; Rundgren, 1998; Caseldine et al., 2003, 2006; Hallsdóttir and Caseldine, 2005), when climate was relatively warm (Langdon et al., 2010)

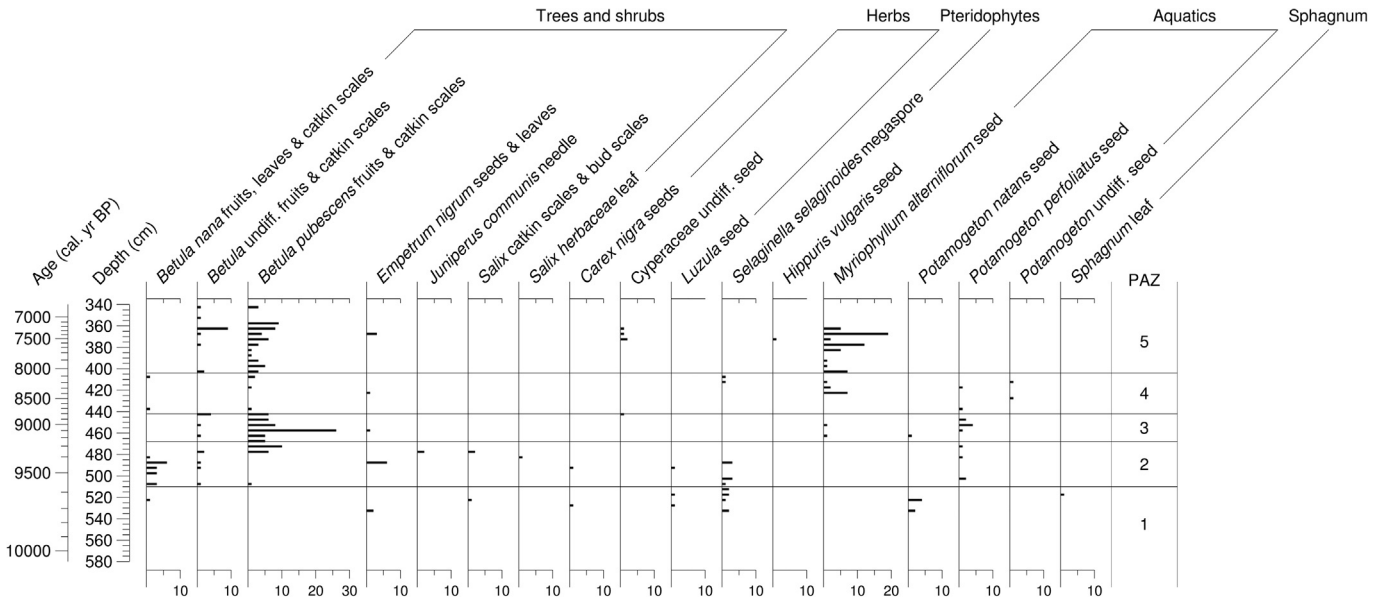

Fig. 6. Plant macrofossil diagram for Kagaðarhóll. Concentrations in 50 mL of sediment.

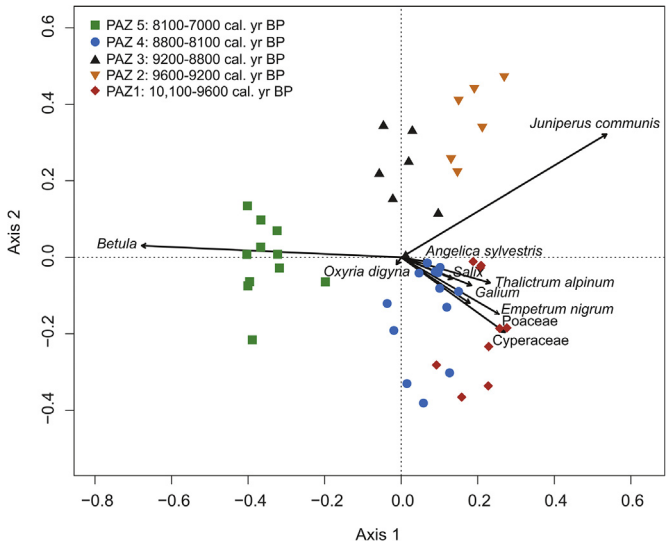

Fig. 7. Principal component analysis of terrestrial pollen from Kagaðarhóll.

and environmental conditions probably favoured *Juniperus communis* over *Betula pubescens* (Eddudóttir et al., 2015). A decrease in pollen from dwarf shrubs, graminoids and other herbs (Figs. 3, 4 and 7) also reflects the transition to a new vegetation community. This period is characterised by environmental instability, indicated by relatively high sedimentation rate (Fig. 2) and large minerogenic input into the lake, as suggested by relatively high and variable DBD (>0.16 g cm^{-3}) and MS. Organic matter (<30%), %TC (~8–12%) and %TN (~0.8–1.2%) are relatively low and δ^{13}C values decrease from −18.6 to −20.6‰. Although the lowest C/N ratios in the record occur during this period, values of 14.2–15.9 (Fig. 8) show that terrestrial organic matter contributed a significant component to the sediment (Meyers and Lallier-Vergès, 1999). The TLP PAR (~3200–6400 grains cm^{-2} yr^{-1}) is the highest during this period, and the TLP concentration is also high (~26,000–50,000 grains cm^{-3}) (Fig. 4), suggesting warm conditions favourable for pollen production.

Small mean *Betula* pollen diameters (~18 ± 1 μm) c. 9600–9200 cal. yr BP (Fig. 5) indicate that *Betula nana* was still the dominant *Betula* species, although *Betula pubescens* macrofossils appear in the record c. 9300 cal. yr BP (Fig. 6). The percentage of non-triporate *Betula* pollen ranges between 2 and 9% during this period (Fig. 4) and is above 3% in most of the pollen samples. A high proportion of non-triporate pollen indicates the presence of hybrid individuals of *Betula nana* and *Betula pubescens*. Modern individuals of *Betula nana* and *Betula pubescens* in Iceland produce on average 2.4% and 0.7% of non-triporate pollen, respectively. In contrast, hybrid individuals of the two species produce about 12.2% non-triporate pollen (Karlsdóttir et al., 2008). The relatively high percentages of non-triporate *Betula* pollen indicate some hybridisation between the two species during the early Holocene as has been recorded at other sites in Iceland (Karlsdóttir et al., 2009, 2012; Karlsdóttir, 2014; Eddudóttir et al., 2015, 2016).

5.2. Early birch woodland development (c. 9200–8800 cal. yr BP)

Birch woodland development is indicated by increased importance of *Betula* in the pollen assemblage c. 9200 cal. yr BP (PAZ 3; Fig. 7). The *Betula* PAR increases to >1000 grains cm^{-2} yr^{-1} after c. 9200 cal. yr BP (Fig. 4) and the relative abundance to >40% of TLP c. 9100 cal. yr BP (Fig. 3). This corresponds to a decrease in *Juniperus communis* pollen to ≤35% of TLP, probably reflecting competition for space with *Betula pubescens* and the effects of an increasingly closed canopy upon the shade intolerant *Juniperus communis* (Thomas et al., 2007). Mean *Betula* diameters increase to ~20 ± 1 μm (Fig. 5), indicating an increased importance of *Betula pubescens* pollen (Mäkelä, 1996). As woodland developed, environmental stability increased, resulting in less minerogenic material deposited in the lake, which is reflected in lower values of DBD (0.13–0.19 g cm^{-3}) and MS. This change in sediment characteristics is reflected in the sedimentation rate that decreases c. 9200 cal. yr BP (Fig. 2). Organic matter proxies show an increase in %TC (14.7–20.9%) and C/N (13.3–14.7), while δ^{13}C decreases (−20.3 to −23.7‰) (Fig. 8). Terrestrial plants in Icelandic lakes have δ^{13}C values that are significantly lower (−24.4 to −30.9‰) than those of aquatic plants (−11,5 to −15,1‰; Wang and Wooller, 2006). Hence, the decrease in δ^{13}C, accompanied by relatively high C/N ratios may

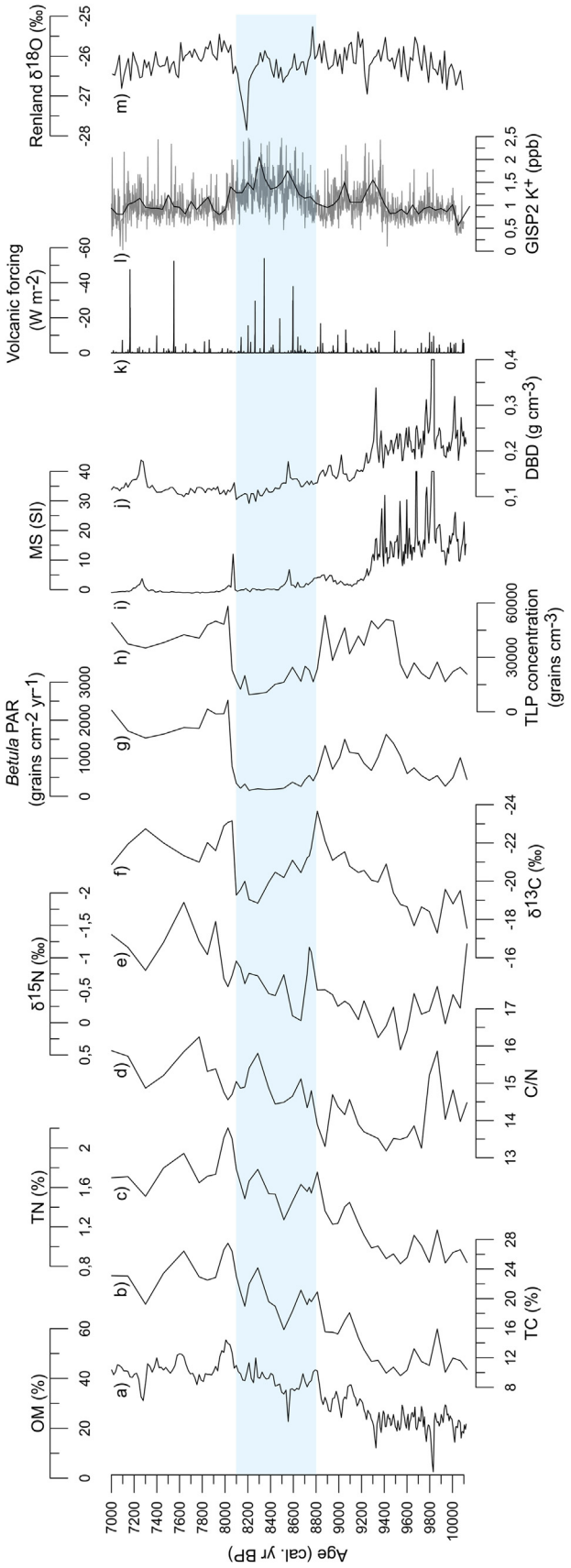

Fig. 8. Organic and physical properties of the Kagaðarhóll sediments compared with selected proxies from Greenland ice core records. a) Organic matter (OM), b) total carbon (%TC), c) total nitrogen (%TN), d) C/N ratio, e) nitrogen isotope ratio ($\delta^{15}N$), f) carbon isotope ratio ($\delta^{13}C$), g) *Betula* PAR, h) total land pollen (TLP) concentration, i) Magnetic susceptibility (MS) showing values below 40 for clarity, j) dry bulk density (DBD) showing values below 0.4 g cm^{-3} for clarity, k) Volcanic forcing based on the GISP2 sulfate record (Kobashi et al., 2017), l) GISP2 K^+, showing values ≤2.5 ppb for clarity, black line represents 50 year mean values (Mayewski et al., 1997), and m) Renland ice-core $\delta^{18}O$ record, 20 year average, uplift corrected (Vinther et al., 2009).

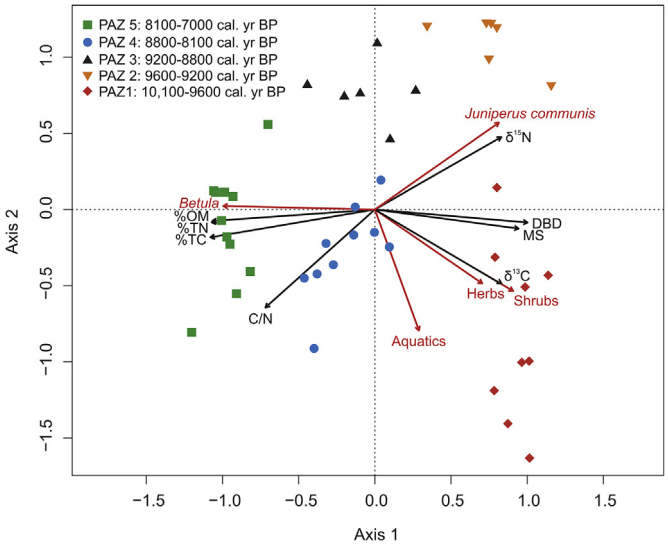

Fig. 9. Principal component analysis of organic and physical properties and pollen from the Kagaðarhóll sediments.

represent an increase in terrestrial input into the lake as woodland encroached upon the area. This is supported by an increase in *Betula pubescens* macrofossils in the sediment during this period (Fig. 6). This stage of woodland development is associated with a period of warm climate in northern Iceland (e.g. Caseldine et al., 2006; Langdon et al., 2010; Eddudóttir et al., 2015).

5.3. Cooling climate (c. 8800–8100 cal. yr BP)

The progression from *Juniperus communis* scrub to *Betula pubescens* woodland was stalled by external factors c. 8800 cal. yr BP, prompting a change towards more open landscape for c. 700 years. A change in the pollen assemblage is interpreted as a change in vegetation community c. 8800 cal. yr BP (Fig. 7), characterised by an increase in Poaceae and Cyperaceae and a further decrease in *Juniperus communis* pollen (Fig. 3). The *Betula* PAR drops below 600 grains cm^{-2} yr^{-1} (Fig. 4) and the relative abundance of *Betula* pollen decreases to <45% of TLP c. 8800 cal. yr BP and <32% after c. 8700 cal. yr BP (Fig. 3). The drop in *Betula* pollen indicates a decrease in pollen deposition from *Betula* species. Despite a decrease in *Betula* pollen accumulation, mean *Betula* pollen diameters remain ~20 ± 1 μm (Fig. 5), suggesting that *Betula pubescens* remained a part of the vegetation community and was not replaced by *Betula nana*. The increase in grass and sedge pollen and decline in *Betula* pollen suggests a more open landscape around the lake as woodland retreated (Figs. 3 and 7). These changes in the pollen assemblage are also recorded in a previous (lower resolution) palynological reconstruction from the same lake (Vasari, 1972; Vasari and Vasari, 1990).

The low concentration and PAR of terrestrial pollen (Figs. 4 and 8) during this period suggests a decrease in pollen production of most terrestrial plants. This is reflected in an increase in the relative abundance of Poaceae and Cyperaceae pollen (Fig. 3), while PARs of the two pollen taxa do not show significant increases (Fig. 4). The

changes in the pollen assemblage may have been caused by lower spring and summer temperatures hindering the reproduction of *Betula pubescens* (Pichugina, 1971) and possibly other taxa. Colder conditions may have caused a shift towards a period of vegetative reproduction by plants. For instance, following damage or stress, *Betula pubescens* can reproduce by sprouting from basal buds or regenerate from stems (Kauppi et al., 1987; Verwijst, 1988). Prior to c. 8800 cal. yr BP, most of the plant macrofossils found in the sediment are *Betula pubescens* catkin scales and fruits, however between c. 8800 and 8100 cal. yr BP very few terrestrial plant macrofossils are recorded (Fig. 6). This, along with the decrease in pollen deposition, may indicate a drop in seed production by terrestrial plants. Higher $\delta^{13}C$ values are recorded c. 8700 cal. yr BP, with the highest values between c. 8400 and 8100 cal. yr BP (−18.9 to −20.5‰). The C/N ratio increases slightly during the same period from 14.4 to 15.1 (Fig. 8). This coincides with the lowest input of land pollen (TLP) into the lake (Fig. 4), and an increase in macrofossils of the aquatic taxon *Myriophyllum alterniflorum* (Fig. 6). The increase in aquatic plant macrofossils and decreased deposition of terrestrial plant pollen and macrofossils in the sediment would lead to higher $\delta^{13}C$ values in the sediment closer to the $\delta^{13}C$ of aquatic plants (−11.5 to −15.1‰), than terrestrial plants (−24,4 to −30,9‰; Wang and Wooller, 2006).

Environmental stability at Kagaðarhóll increased from c. 8800 to 8100 cal. yr BP, despite a response by the vegetation community suggesting colder climate. Minerogenic input into the lake decreased during the period, indicated by declining DBD ($\leq$0.14 g cm^{-3}) and MS values, with the exception of a tephra layer deposited c. 8550 cal. yr BP (Fig. 8). The data show a progression from more minerogenic to more organic sediment with time, without a regression to more unstable conditions (Fig. 9). This is contrary to several other studies in Iceland that have found evidence of increased soil erosion in the wake of cooling climate c. 8700 cal. yr BP at highland sites (Larsen et al., 2012; Geirsdóttir et al., 2013; Gunnarsson, 2016; Harning et al., 2018). The tall vegetation cover around the Kagaðarhóll lake and the position of the lake in the lowlands may be the reason for the different response. This may indicate that environmental instability increased in the highlands, while stable conditions prevailed in the lowlands during this period.

Indications of colder spring/summer temperatures and possible glacier advances, corresponding with the changes in vegetation at Kagaðarhóll, are recorded in Lake Hvítárvatn in the western highlands of Iceland beginning c. 8700 cal. yr BP, with two rapid cooling episodes at c. 8500 and 8200 cal. yr BP (Larsen et al., 2012). Chironomid-inferred July temperatures (July CI-T) from nearby Tröllaskagi peninsula show a gradual cooling between c. 9000 and 8100 cal. yr BP, with a drop in July CI-T c. 8500 cal. yr BP. However, cooling is not evident in the pollen record from the sites in Tröllaskagi. On the contrary, the relative abundance of *Betula* increases after c. 8400 cal. yr BP (Caseldine et al., 2006). Changes in pollen assemblages similar to those at Kagaðarhóll are recorded at Vatnskotsvatn in Skagafjörður, east of Húnaflói between c. 8300 and 8000 cal. yr BP, where development of birch woodland was interrupted by reoccurrence of *Juniperus-Salix-Betula nana* heath (Hallsdóttir, 1995). Records that show a response to long-term cooling c. 8800–7900 cal. yr BP are concentrated in northwestern and western Iceland, although it should be noted that most available palaeoecolgical and environmental records covering the period are from northern Iceland. A short, sharp cooling with a change to cooler winter and spring temperatures is observed in the only record available from eastern Iceland c. 8200–8000 cal. yr BP (Striberger et al., 2012), which shows more similarities to responses observed in northern Europe (Rohling and Pälike, 2005; Seppä et al., 2007, 2009) than those in northwestern and western Iceland. Marine records northwest and west of Iceland show a long period of cooling, beginning c. 8750–8600 cal. yr BP, and intensifying c. 8200 cal. yr BP (Knudsen et al., 2004; Ólafsdóttir et al., 2010). A shorter cold period, accompanied by an increase in sea-ice c. 8300–8100 cal. yr BP, indicating decreased strength of the Irminger current, is recorded north of Iceland (Ran et al., 2006). Other marine records around Iceland show a relatively minor cooling associated with the 8.2 ka event (e.g. Andersen et al., 2004; Castañeda et al., 2004; Ran et al., 2006; Jiang et al., 2015).

5.4. Woodland recovery (c. 8100–7000 cal. yr BP)

Betula becomes the dominant pollen taxon in the terrestrial pollen assemblage after c. 8100 cal. yr BP when *Betula pubescens* woodland begins to recover (Figs. 3, 4 and 7). A sharp increase in *Betula* pollen is recorded after c. 8100 cal. yr BP, as the PAR increases from ~200 to >2000 grains cm^{-2} yr^{-1} between c. 8100–8000 cal. yr BP. This change is confirmed by a relative increase of *Betula pollen* from ~30 to 80% of TLP, showing relative changes in pollen taxa abundance, independent of changes in sedimentation rates. Relative abundances and PARs of other pollen taxa decrease, including *Juniperus communis*, *Salix*, Poaceae, Cyperaceae and *Thalictrum alpinum* (Figs. 3 and 4). The change in pollen assemblage occurs within less than a century, indicating a rapid response of the vegetation community to warming climate. A relatively stable woodland community is reflected in the pollen assemblage until the end of the record c. 7000 cal. yr BP (Figs. 3, 4 and 7). The most stable period in the record is characterised by an increase in %OM to >37% and %TC to >19%. The $\delta^{13}C$ decreases to $\leq$ −21‰ and the C/N ratio is 14.6–16.2, probably indicating a greater input of organic terrestrial material into the lake (Figs. 8 and 9). This may be in part due to the reappearance of *Betula pubescens* catkin scales and fruits in the sediment (Fig. 6). This period corresponds to the Holocene Thermal Maximum (HTM), the most stable period of the Holocene in Iceland, lasting until c. 6000–5500 cal. yr BP (Caseldine et al., 2006; Larsen et al., 2012; Striberger et al., 2012; Geirsdóttir et al., 2013; Blair et al., 2015; Eddudóttir et al., 2015, 2016; Eddudóttir, 2016).

5.5. Climate anomalies c. 8800–8000 cal. yr BP

The changes to colder springs/summers documented in the palaeoecological reconstruction from Kagaðarhóll occur c. 8800 ± 110 cal. yr BP (Figs. 3, 4 and 7). Responses to cooling are recorded in other lakes in northwestern and western Iceland c. 8700 cal. yr BP (e.g. Larsen et al., 2012; Geirsdóttir et al., 2013; Harning et al., 2018). The responses manifested in proxies sensitive to spring and summer temperatures in Iceland, such as the *Betula* PAR at Kagaðarhóll (Fig. 8), are similar to proxies that record global climate anomalies c. 8600 and 8000 cal. yr BP (e.g. Rohling and Pälike, 2005; Wanner et al., 2011). A cold temperature anomaly is observed in some records from the Greenland Ice Sheet beginning a few centuries before the more severe 8.2 ka event (Fig. 8; Vinther et al., 2009; Kobashi et al., 2017). The period is characterised by a complex pattern of climate change in the North Atlantic region and beyond when remnants of large ice sheets were still present in the Northern Hemisphere (Mayewski et al., 2004). Rohling and Pälike (2005) identified a longer period of climate anomalies recorded in summer proxies from c. 8600 cal. yr BP, distinct from a shorter event affecting winter and early spring temperatures beginning c. 8300 cal. yr BP. The shorter event is recorded in pollen based temperature reconstructions in Northern Europe and indicates colder winters and early springs between c. 8300 and 8000 cal. yr BP in response to freshwater input into the North Atlantic.

However, pollen records from northern Fennoscandia show little or no evidence of colder conditions in May and June (Seppä et al., 2007, 2009).

Atmospheric circulation changes are observed in records c. 8650–8000 cal. yr BP, such as expansion of the polar vortex, suggested by records of potassium ions (Fig. 8) and dust in the GISP2 core from Greenland (Taylor et al., 1992, 1993; Mayewski et al., 1997), weakening of the African, Indian and Asian monsoons between c. 8500 and 8000 cal. yr BP (Gasse, 2000; Hong et al., 2003; Yuan et al., 2004), and migration of the Intertropical Convergence Zone (ITCZ) (Haug et al., 2001). Several drivers have been proposed for cooling climate during this period; i.e. changes in solar output, meltwater discharge from the Laurentide Ice Sheet and volcanism. Although a solar output minima is recorded c. 8400 cal. yr BP (Steinhilber et al., 2009) it is not considered enough to explain the observed changes in climate (Wanner et al., 2011). Episodic cooling of the Irminger Current occurred c. 9500–8100 cal. yr BP due to fluxes of freshwater from the Laurentide Ice Sheet into the North Atlantic (Jennings et al., 2011). Three pulses of freshwater from the Laurentide Ice Sheet are recorded, peaking c. 8636, 8565 and 8147 cal. yr BP (Jennings et al., 2015). This coincides with three events of relative sea level increase recorded in Scotland between c. 8760 to 8218 cal. yr BP, each lasting 105–130 years (Lawrence et al., 2016). The first two events are linked to the opening of the Tyrrell Sea and the last one with the drainage of lakes Agassiz and Ojibway. All events are part of a series of freshwater events originating from Hudson Bay and Hudson Strait between c. 11,500 and 8000 cal. yr BP (Jennings et al., 2015). The period between c. 9000–8000 cal. yr BP is also characterised by large volcanic eruptions, with the highest occurrence of volcanic activity during the Holocene recorded in the Greenland Ice Sheet c. 8600–8000 cal. yr BP (Fig. 8; Kobashi et al., 2017). There is evidence of intensified volcanic activity in the Kamchatka Peninsula during this period (Braitseva et al., 1995, 1997), including the Karymsky caldera eruption c. 8770 ± 210 cal. yr BP (7889 ± 67 ^{14}C yr) and Kuril Lake-Iliinsky eruption c. 8460 ± 60 cal. yr BP (7666 ± 19 ^{14}C yr; Braitseva et al., 1997), an extremely large eruption that produced ~120–140 km^3 of pyroclastic material (Braitseva et al., 1997). Furthermore the largest Holocene lava on Earth, the Þjórsárhraun lava was formed c. 8590 ± 170 cal. yr BP (7800 ± 60 ^{14}C yr; Hjartarson, 1988). The minimum size of the eruptive material produced is estimated to be ~25 km^3 DRE (dense rock equivalent) (Hjartarson, 2011). The recent, much smaller (1.2 km^3 DRE; Bonny et al., 2018), Holuhraun eruption originating from the same volcanic system, has demonstrated that high amounts of SO_2 and aerosol particulate matter are emitted from effusive eruptions from the system (Ilyinskaya et al., 2017). Model simulations of volcanic forcing have suggested that a large volcanic eruption can cause climate cooling and sea-ice expansion that can last for over a century (Kobashi et al., 2017; Miller et al., 2012), resulting in prolonged periods of cold summers (Miller et al., 2012). A succession of large eruptions can therefore potentially cause centuries-long cold periods (Kobashi et al., 2017), such as the one observed in the Kagaðarhóll record.

The pollen record from Kagaðarhóll suggests relatively stable conditions at the site between c. 8800 and 8100 cal. yr BP, despite a change in vegetation community. The early response of the palaeoenvironmental proxies in northwestern and western Iceland to colder spring and summer temperatures is probably due to northwestern Iceland's marginal location and the region's sensitivity to ocean currents, showing more similarities to responses in some marine records (Knudsen et al., 2004; Ólafsdóttir et al., 2010) and Greenland ice core records (Fig. 8; Vinther et al., 2009; Kobashi et al., 2017) than terrestrial records from Northern Europe (Seppä et al., 2007, 2009). This demonstrates the ability of Icelandic palaeoenvironmental reconstructions to capture signals of North Atlantic climate variability.

6. Conclusions

The pollen record from Kagaðarhóll clearly demonstrates a change in vegetation community beginning c. 8800 cal. yr BP. During the period c. 8800–8100 cal. yr BP, cold climate probably interrupted the vegetation succession from *Juniperus communis* scrub to *Betula pubescens* woodland that had taken place during a relatively warm early Holocene c. 10.100–8800 cal. yr BP. The record shows a significant decrease in pollen production from terrestrial plants, especially *Betula pubescens* c. 8800–8100 cal. yr BP, probably reflecting colder spring and/or summer temperatures. Despite a colder climate, proxies of organic and physical properties of the sediment do not indicate increased instability, i.e. soil erosion in the area around the lake, showing the stability of the established *Betula pubescens* woodland and the resilience of the more open vegetation community in response to colder climate. The birch woodland shows quick recovery with warming climate between c. 8100 and 8000 cal. yr BP. The results show the potential of terrestrial multi-proxy records from Iceland for reconstructions of climate variability in the North Atlantic.

Acknowledgements

The authors would like to thank Ólafur Eggertsson, Friðþór Sófus Sigurmundsson and Þorsteinn Jónsson for assistance in the field. Jessica Lynn Till is thanked for proofreading the manuscript. We would like to thank Olga Kolbrún Vilmundardóttir and Scott John Riddell for discussions on vegetation communities. We would like to thank two anonymous reviewers for their valuable comments and suggestions. The Blönduvirkjun hydropower plant kindly hosted us during fieldwork. The research was funded by the Landsvirkjun Energy Research Fund, the University of Iceland Eimskip Fund, the University of Iceland Research Fund, and the Icelandic Research Fund (grant no. 141842-051).

Appendix A. Supplementary data

Supplementary data related to this article can be found at https://doi.org/10.1016/j.quascirev.2018.07.017.

References

Aaby, B., Berglund, B.E., 1986. Characterization of Peat and lake Deposits. Handbook of Holocene palaeoecology and palaeohydrology John Wiley & Sons, Chichester, pp. 231–246.

Alley, R.B., Ágústsdóttir, A.M., 2005. The 8k event: cause and consequences of a major Holocene abrupt climate change. Quat. Sci. Rev. 24, 1123–1149. https://doi.org/10.1016/j.quascirev.2004.12.004.

Alley, R.B., Mayewski, P.A., Sowers, T., Stuiver, M., Taylor, K.C., Clark, P.U., 1997. Holocene climatic instability: a prominent, widespread event 8200 yr ago. Geology 25, 483–486. https://doi.org/10.1130/0091-7613(1997)025<0483:hciapw>2.3.co;2.

Andersen, C., Koç, N., Moros, M., 2004. A highly unstable Holocene climate in the subpolar North Atlantic: evidence from diatoms. Quat. Sci. Rev. 23, 2155–2166.

Baldini, J.U., McDermott, F., Fairchild, I.J., 2002. Structure of the 8200-year cold event revealed by a speleothem trace element record. Science 296, 2203–2206.

Bamberg, A., Rosenthal, Y., Paul, A., Heslop, D., Mulitza, S., Rühlemann, C., Schulz, M., 2010. Reduced North Atlantic central water formation in response to early Holocene ice-sheet melting. Geophys. Res. Lett. 37.

Barber, D.C., Dyke, A., Hillaire-Marcel, C., Jennings, A.E., Andrews, J.T., Kerwin, M.W., Bilodeau, G., McNeely, R., Southon, J., Morehead, M.D., 1999. Forcing of the cold event of 8,200 years ago by catastrophic drainage of Laurentide lakes. Nature 400, 344–348.

Bengtsson, L., Enell, M., 1986. Chemical analysis. In: Berglund, B.E. (Ed.), Handbook of Holocene Palaeoecology and Palaeohydrology. John Wiley & Sons, Chichester,

pp. 423–451.
Bennett, K.D., 2016. Catalogue of Pollen Types. http://www.chrono.qub.ac.uk/pollen/pc-intro.html.
Birks, H.J.B., 1973. Modern pollen studies in some arctic and alpine environments. In: Birks, H.J.B., West, R.G. (Eds.), Quaternary Plant Ecology. Blackwell, Oxford, pp. 143–168.
Birks, H.H., Bjune, A.E., 2010. Can we detect a west Norwegian tree line from modern samples of plant remains and pollen? Results from the DOORMAT project. Veg. Hist. Archaeobotany 19, 325–340.
Björck, S., Persson, T., Kristersson, I., 1978. Comparison of two concentration methods for pollen in minerogenic sediments. GFF 100, 107–111.
Blaauw, M., 2010. Methods and code for 'classical' age-modelling of radiocarbon sequences. Quat. Geochronol. 5, 512–518. https://doi.org/10.1016/j.quageo.2010.01.002.
Blair, C.L., Geirsdottir, A., Miller, G.H., 2015. A high-resolution multi-proxy lake record of Holocene environmental change in southern Iceland. J. Quat. Sci. 30, 281–292.
Bonny, E., Thordarson, T., Wright, R., Höskuldsson, A., Jónsdóttir, I., 2018. The volume of lava erupted during the 2014 to 2015 eruption at Holuhraun, Iceland: a comparison between satellite- and ground-based measurements. J. Geophys. Res.: Solid Earth. https://doi.org/10.1029/2017JB015008.
Brady, N.C., Weil, R.R., 1996. Elements of the Nature and Properties of Soils, second ed. Pearson Prentice-Hall, Upper Saddle River.
Braitseva, O.A., Melekestsev, I.V., Ponomareva, V.V., Sulerzhitsky, L., 1995. Ages of calderas, large explosive craters and active volcanoes in the Kuril-Kamchatka region, Russia. Bull. Volcanol. 57, 383–402.
Braitseva, O.A., Ponomareva, V.V., Sulerzhitsky, L.D., Melekestsev, I.V., Bailey, J., 1997. Holocene key-marker tephra layers in Kamchatka, Russia. Quat. Res. 47, 125–139.
Caseldine, C., Geirsdóttir, Á., Langdon, P., 2003. Efstadalsvatn–a multi-proxy study of a Holocene lacustrine sequence from NW Iceland. J. Paleolimnol. 30, 55–73.
Caseldine, C., Langdon, P., Holmes, N., 2006. Early Holocene climate variability and the timing and extent of the Holocene thermal maximum (HTM) in northern Iceland. Quat. Sci. Rev. 25, 2314–2331.
Castañeda, I.S., Smith, L.M., Kristjánsdóttir, G.B., Andrews, J.T., 2004. Temporal changes in Holocene δ18O records from the northwest and central North Iceland Shelf. J. Quat. Sci. 19, 321–334.
Dearing, J., 1994. Environmental Magnetic Susceptibility: Using the Bartington MS2 System. Chi Publishing, Kenilworth.
Eddudóttir, S.D., 2016. Holocene Environmental Change in Northwest Iceland. PhD dissertation. University of Iceland.
Eddudóttir, S.D., Erlendsson, E., Gísladóttir, G., 2015. Life on the periphery is tough: vegetation in Northwest Iceland and its responses to early-Holocene warmth and later climate fluctuations. Holocene 25, 1437–1453.
Eddudóttir, S.D., Erlendsson, E., Gísladóttir, G., 2017. Effects of the Hekla 4 tephra on vegetation in northwest Iceland. Veg. Hist. Archaeobotany 26 (4), 389–402. https://doi.org/10.1007/s00334-017-0603-5.
Eddudóttir, S.D., Erlendsson, E., Tinganelli, L., Gísladóttir, G., 2016. Climate change and human impact in a sensitive ecosystem: the Holocene environment of the Northwest Icelandic highland margin. Boreas 45, 715–728.
Erlendsson, E., 2007. Environmental Change Around the Time of the Norse Settlement of Iceland. PhD dissertation. University of Aberdeen.
Faegri, K., Kaland, P.E., Krzywinski, K., 1989. Textbook of Pollen Analysis, fourth ed. John Wiley & Sons, New York.
Gasse, F., 2000. Hydrological changes in the african tropics since the last glacial maximum. Quat. Sci. Rev. 19, 189–211.
Geirsdóttir, Á., Miller, G.H., Axford, Y., Ólafsdóttir, S., 2009. Holocene and latest Pleistocene climate and glacier fluctuations in Iceland. Quat. Sci. Rev. 28, 2107–2118.
Geirsdóttir, Á., Miller, G.H., Larsen, D.J., Ólafsdóttir, S., 2013. Abrupt Holocene climate transitions in the northern North Atlantic region recorded by synchronized lacustrine records in Iceland. Quat. Sci. Rev. 70, 48–62. https://doi.org/10.1016/j.quascirev.2013.03.010.
Grimm, E.C., 2011. TILIA 1.7.16. Illinois state museum, Springfield.
Gudmundsdóttir, E.R., Larsen, G., Eiríksson, J., 2011. Two new Icelandic tephra markers: the Hekla Ö tephra layer, 6060 cal. yr BP, and Hekla DH tephra layer, ~6650 cal. yr BP. Land-sea correlation of mid-Holocene tephra markers. Holocene 21, 629–639.
Gunnarsson, S., 2016. Holocene Climate and Landscape Evolution in the West Central Highlands, Iceland. MSc dissertation. University of Iceland.
Hallsdóttir, M., 1987. Pollen Analytical Studies of Human Influence on Vegetation in Relation to the Landnám Tephra Layer in Southwest Iceland. PhD Thesis. Lund University.
Hallsdóttir, M., 1995. On the pre-settlement history of Icelandic vegetation. Buvisindi 9, 19–29.
Hallsdóttir, M., Caseldine, C.J., 2005. The Holocene vegetation history of Iceland, state-of-the-art and future research. In: Caseldine, C., Russel, A., Harðardóttir, J., Knudsen, Ó (Eds.), Iceland – Modern Processes and Past Environments. Elsevier, Amsterdam, pp. 319–334.
Hansen, B., Østerhus, S., 2000. North Atlantic–Nordic seas exchanges. Prog. Oceanogr. 45, 109–208.
Harning, D.J., Geirsdóttir, Á., Miller, G.H., 2018. Punctuated Holocene climate of Vestfirðir, Iceland, linked to internal/external variables and oceanographic conditions. Quat. Sci. Rev. 189, 31–42. https://doi.org/10.1016/j.quascirev.2018.04.009.
Haug, G.H., Hughen, K.A., Sigman, D.M., Peterson, L.C., Röhl, U., 2001. Southward migration of the intertropical convergence zone through the Holocene. Science 293, 1304–1308.
Hjartarson, Á., 1988. Þjórsárhraunið mikla, stærsta nútímahraun jarðar. Náttúrufræðingurinn 58, 1–16.
Hjartarson, Á., 2011. Víðáttumesta hraun Íslands. Náttúrufræðingurinn 81, 37–49.
Hong, Y.T., Hong, B., Lin, Q.H., Zhu, Y.X., Shibata, Y., Hirota, M., Uchida, M., Leng, X.T., Jiang, H.B., Xu, H., 2003. Correlation between indian ocean summer monsoon and North Atlantic climate during the Holocene. Earth Planet Sci. Lett. 211, 371–380.
Huntley, B., Birks, H.J.B., 1983. An Atlas of Past and Present Pollen Maps for Europe: 0–13000 Years Ago. Cambridge University Press, Cambridge.
Ilyinskaya, E., Schmidt, A., Mather, T.A., Pope, F.D., Witham, C., Baxter, P., Jóhannsson, T., Pfeffer, M., Barsotti, S., Singh, A., Sanderson, P., Bergsson, B., McCormick Kilbride, B., Donovan, A., Peters, N., Oppenheimer, C., Edmonds, M., 2017. Understanding the environmental impacts of large fissure eruptions: aerosol and gas emissions from the 2014–2015 Holuhraun eruption (Iceland). Earth Planet Sci. Lett. 472, 309–322.
Jennings, A., Andrews, J., Wilson, L., 2011. Holocene environmental evolution of the se Greenland shelf north and south of the Denmark strait: irminger and east Greenland current interactions. Quat. Sci. Rev. 30, 980–998.
Jennings, A., Andrews, J., Pearce, C., Wilson, L., Ólafsdóttir, S., 2015. Detrital carbonate peaks on the Labrador shelf, a 13–7ka template for freshwater forcing from the Hudson Strait outlet of the Laurentide Ice Sheet into the subpolar gyre. Quat. Sci. Rev. 107, 62–80.
Jiang, H., Muscheler, R., Björck, S., Seidenkrantz, M.-S., Olsen, J., Sha, L., Sjolte, J., Eiríksson, J., Ran, L., Knudsen, K.-L., 2015. Solar forcing of Holocene summer sea-surface temperatures in the northern North Atlantic. Geology 43, 203–206.
Jóhannesson, H., 2014. Jarðfræðikort af Íslandi 1:600 000 Berggrunnur (Geological Map of Iceland 1:600 000 Bedrock Geology). Náttúrufræðistofnun Íslands, Garðabær.
Kardjilov, M., Gisladottir, G., Gislason, S., 2006. Land degradation in northeastern Iceland: present and past carbon fluxes. Land Degrad. Dev. 17, 401–417.
Karlsdóttir, L., 2014. Hybridisation of Icelandic Birch in the Holocene Reflected in Pollen. PhD dissertation. University of Iceland.
Karlsdóttir, L., Hallsdóttir, M., Thórsson, A.T., Anamthawat-Jónsson, K., 2008. Characteristics of pollen from natural triploid Betula hybrids. Grana 47, 52–59.
Karlsdóttir, L., Hallsdóttir, M., Thórsson, Æ.T., Anamthawat-Jónsson, K., 2009. Evidence of hybridisation between Betula pubescens and B. nana in Iceland during the early Holocene. Rev. Palaeobot. Palynol. 156, 350–357.
Karlsdóttir, L., Hallsdóttir, M., Thórsson, Æ.T., Anamthawat-Jónsson, K., 2012. Early Holocene hybridisation between Betula pubescens and B. nana in relation to birch vegetation in Southwest Iceland. Rev. Palaeobot. Palynol. 181, 1–10.
Kauppi, A., Rinne, P., Ferm, A., 1987. Initiation, structure and sprouting of dormant basal buds in Betula pubescens. Flora 179.
Knudsen, K., Jiang, H., Jansen, E., Eirıksson, J., Heinemeier, J., Seidenkrantz, M.-S., 2004. Environmental changes off North Iceland during the deglaciation and the Holocene: foraminifera, diatoms and stable isotopes. Mar. Micropaleontol. 50, 273–305.
Kobashi, T., Menviel, L., Jeltsch-Thömmes, A., Vinther, B.M., Muscheler, R., Nakaegawa Pfister, P.L., Döring, M., Leuenberger, M., Wanner, H., 2017. Volcanic influence on centennial to millennial Holocene Greenland temperature change. Sci. Rep. 7, 1441.
Langdon, P.G., Leng, M., Holmes, N., Caseldine, C.J., 2010. Lacustrine evidence of early-Holocene environmental change in northern Iceland: a multiproxy palaeoecology and stable isotope study. Holocene 20, 205–214.
Larsen, D.J., Miller, G.H., Geirsdóttir, Á., Ólafsdóttir, S., 2012. Non-linear Holocene climate evolution in the North Atlantic: a high-resolution, multi-proxy record of glacier activity and environmental change from Hvítárvatn, central Iceland. Quat. Sci. Rev. 39, 14–25.
Larsen, D.J., Miller, G.H., Geirsdóttir, Á., Thordarson, T., 2011. A 3000-year varved record of glacier activity and climate change from the proglacial lake Hvítárvatn, Iceland. Quat. Sci. Rev. 30, 2715–2731.
Lawrence, T., Long, A.J., Gehrels, W.R., Jackson, L.P., Smith, D.E., 2016. Relative sea-level data from southwest Scotland constrain meltwater-driven sea-level jumps prior to the 8.2 kyr BP event. Quat. Sci. Rev. 151, 292–308.
Mäkelä, E.M., 1996. Size distinctions between Betula pollen types—a review. Grana 35, 248–256.
Mayewski, P.A., Meeker, L.D., Twickler, M.S., Whitlow, S., Yang, Q., Lyons, W.B., Prentice, M., 1997. Major features and forcing of high-latitude northern hemisphere atmospheric circulation using a 110,000-year-long glaciochemical series. J. Geophys. Res.: Oceans 102, 26345–26366.
Mayewski, P.A., Rohling, E.E., Stager, J.C., Karlén, W., Maasch, K.A., Meeker, L.D., Meyerson, E.A., Gasse, F., van Kreveld, S., Holmgren, K., 2004. Holocene climate variability. Quat. Res. 62, 243–255.
Meyers, P.A., Lallier-Vergès, E., 1999. Lacustrine sedimentary organic matter records of Late Quaternary paleoclimates. J. Paleolimnol. 21, 345–372.
Miller, G.H., Geirsdóttir, Á., Zhong, Y., Larsen, D.J., Otto-Bliesner, B.L., Holland, M.M., Bailey, D.A., Refsnider, K.A., Lehman, S.J., Southon, J.R., 2012. Abrupt onset of the Little Ice Age triggered by volcanism and sustained by sea-ice/ocean feedbacks. Geophys. Res. Lett. 39.
Moore, P.D., Webb, J.A., Collison, M.E., 1991. Pollen Analysis. Blackwell scientific publications, Oxford.
Nakagawa, T., Brugiapaglia, E., Digerfeldt, G., Reille, M., Beaulieu, J.-L.D., Yasuda, Y., 1998. Dense-media separation as a more efficient pollen extraction method for

use with organic sediment/deposit samples: comparison with the conventional method. Boreas 27, 15–24. https://doi.org/10.1111/j.1502-3885.1998.tb00864.x.
Oksanen, J., Blanchet, F.G., Kindt, R., Legendre, P., Minchin, P.R., O'Hara, R.B., Simpson, G.L., Solymos, P., Stevens, M.H.H., Wagner, H., 2016. Vegan: Community Ecology Package, R Package Version 2.3-3 Edn.
Ólafsdóttir, S., Jennings, A.E., Geirsdóttir, Á., Andrews, J., Miller, G.H., 2010. Holocene variability of the North Atlantic Irminger current on the south-and northwest shelf of Iceland. Mar. Micropaleontol. 77, 101–118.
Pichugina, N.P., 1971. Effect of ecological factors on seed formation in certain interspecific birch hybrids. Ecologiya: Sov. J. Ecol. 6, 89–91.
Ran, L., Jiang, H., Knudsen, K.L., Eiríksson, J., Gu, Z., 2006. Diatom response to the Holocene climatic optimum on the North Icelandic shelf. Mar. Micropaleontol. 60, 226–241.
Rasmussen, S.O., Andersen, K.K., Svensson, A.M., Steffensen, J.P., Vinther, B.M., Clausen, H.B., Siggaard-Andersen, M.L., Johnsen, S.J., Larsen, L.B., Dahl-Jensen, D., Bigler, M., Röthlisberger, R., Fischer, H., Goto-Azuma, Hansson ME., Ruth, U., 2006. A new Greenland ice core chronology for the last glacial termination. J. Geophys. Res.: Atmosphere 111. D06102.
Rohling, E.J., Pälike, H., 2005. Centennial-scale climate cooling with a sudden cold event around 8,200 years ago. Nature 434, 975.
Rundgren, M., 1998. Early-Holocene vegetation of northern Iceland: pollen and plant macrofossil evidence from the Skagi peninsula. Holocene 8, 553–564.
Schomacker, A., Brynjólfsson, S., Andreassen, J.M., Gudmundsdóttir, E.R., Olsen, J., Odgaard, B.V., Håkansson, L., Ingólfsson, Ó., Larsen, N.K., 2016. The Drangajökull ice cap, northwest Iceland, persisted into the early-mid Holocene. Quat. Sci. Rev. 148, 68–84.
Seppä, H., Birks, H.J.B., Giesecke, T., Hammarlund, D., Alenius, T., Antonsson, K., Bjune, A.E., Heikkilä, M., MacDonald, G.M., Ojala, A.E.K., 2007. Spatial structure of the 8200 cal yr BP event in northern Europe. Clim. Past Discuss 3, 165–195.
Seppä, H., Bjune, A.E., Telford, R.J., Birks, H., Veski, S., 2009. Last nine-thousand years of temperature variability in Northern Europe. Clim. Past 5, 523–535.
Stefánsson, U., 1962. North Icelandic Waters, Reykjavík.
Steinhilber, F., Beer, J., Fröhlich, C., 2009. Total solar irradiance during the Holocene. Geophys. Res. Lett. 36.
Stockmarr, J., 1971. Tablets with spores used in absolute pollen analysis. Pollen Spores 13, 614–621.
Striberger, J., Björck, S., Holmgren, S., Hamerlík, L., 2012. The sediments of Lake Lögurinn–A unique proxy record of Holocene glacial meltwater variability in eastern Iceland. Quat. Sci. Rev. 38, 76–88.
Taylor, K., Alley, R., Fiacco, J., Grootes, P., Lamorey, G., Mayewski, P., Spencer, M.J., 1992. Ice-core dating and chemistry by direct-current electrical conductivity. J. Glaciol. 38, 325–332.
Taylor, K.C., Lamorey, G.W., Doyle, G.A., Alley, R.B., Grootes, P.M., Mayewski, P.A., White, J.W.C., Barlow, L.K., 1993. The 'flickering switch'of late Pleistocene climate change. Nature 361, 432.
Thomas, P.A., El-Barghathi, M., Polwart, A., 2007. Biological flora of the British isles: Juniperus communis L. J. Ecol. 95, 1404–1440. https://doi.org/10.1111/j.1365-2745.2007.01308.x.
Thorarinsson, S., 1971. The age of the light Hekla tephra layers according to corrected C14–datings. Náttúrufræðingurinn 41, 99–105.
Vasari, Y., 1972. The history of the vegetation in Iceland during the Holocene. In: Vasari, Y., Hyvärinen, H., Hicks, S. (Eds.), Climatic Changes in Arctic Areas during the Last Ten-thousand Years. University of Oulu, Oulu, pp. 239–252.
Vasari, Y., Vasari, A., 1990. L'histoire Holocéne des lacs Islandais. In: Malaurie, J. (Ed.), 102 témoignages en hommage á quarante ans d'études arctiques. Éditions Plon, Paris, pp. 279–293.
Verwijst, T., 1988. Environmental correlates of multiple-stem formation in Betula pubescens ssp. Tortuosa. Vegetatio 76, 29–36. https://doi.org/10.1007/BF00047385.
Vinther, B.M., Buchardt, S.L., Clausen, H.B., Dahl-Jensen, D., Johnsen, S.J., Fisher, D.A., Koerner, R.M., Raynaud, D., Lipenkov, V., Andersen, K.K., 2009. Holocene thinning of the Greenland ice sheet. Nature 461, 385–388.
Wang, Y., Wooller, M.J., 2006. The stable isotopic (C and N) composition of modern plants and lichens from northern Iceland: with ecological and paleoenvironmental implications. Jokull 56, 27–38.
Wanner, H., Solomina, O., Grosjean, M., Ritz, S.P., Jetel, M., 2011. Structure and origin of Holocene cold events. Quat. Sci. Rev. 30, 3109–3123.
Yuan, D., Cheng, H., Edwards, R.L., Dykoski, C.A., Kelly, M.J., Zhang, M., Qing, J., Lin, Y., Wang, Y., Wu, J., 2004. Timing, duration, and transitions of the last interglacial Asian monsoon. Science 304, 575–578.